Majumder, Ritwik and Ghosh, Arindam and Ledwich, Gerard and Zare, Firuz (2009) *Load sharing and power quality enhanced operation of a distributed microgrid.* I. E. T. Renewable Power Generation, 3(2). pp. 109-119.

Load Sharing and Power Quality Enhanced Operation of a Distributed Microgrid

Ritwik Majumder, Arindam Ghosh, Gerard Ledwich and Firuz Zare
School of Engineering Systems
Queensland University of Technology
Brisbane, Qld 4001, Australia.

ABSTRACT: This paper describes control methods for proper load sharing between parallel converters connected in a microgrid and supplied by distributed generators (DGs). It is assumed that the microgrid spans a large area and it supplies loads in both in grid connected and islanded modes. A control strategy is proposed to improve power quality and proper load sharing in both islanded and grid connected modes. It is assumed that each of the DGs has a local load connected to it which can be unbalanced and/or nonlinear. The DGs compensate the effects of unbalance and nonlinearity of the local loads. Common loads are also connected to the microgrid, which are supplied by the utility grid under normal conditions. However during islanding, each of the DGs supplies its local load and shares the common load through droop characteristics. Both impedance and motor loads are considered to verify the system response. The efficacy of the controller has been validated through simulation for various operating conditions using PSCAD. It has been found through simulation that the total Harmonic Distortion (THD) of the of the microgrid voltage is about 10% and the negative and zero sequence component are around 20% of the positive sequence component before compensation. After compensation, the THD remain below 0.5%, whereas, negative and zero sequence components of the voltages remain below 0.02% of the positive sequence component.

Index Terms: Microgrid, Power quality, Non linear and unbalance load, Active and Reactive Power sharing.

I. INTRODUCTION

The interconnection of distributed generators (DGs) to the utility grid through power electronic converters has raised concern about power quality and proper load sharing between different DGs and the grid. Microgrid can generally be viewed as a cluster of distributed generators connected to the main utility grid, usually through some voltage source converter (VSC) based interfaces. Concerning the interfacing of a microgrid to the utility system, an important area of study is to investigate the overall system performance with unbalanced and non linear loads, as these are common in distribution levels. A common practice is to isolate the microgrid from the utility grid by an isolator if the voltage is seriously unbalanced [1]. However when the voltages are not critically unbalanced, the isolator will remain closed, subjecting the microgrid to sustained unbalanced voltages at the point of common coupling (PCC), if no compensating action is taken. Unbalance voltages can cause abnormal operation particularly for sensitive loads and increased losses in motor loads.

Many innovative control techniques have been used for power quality enhanced operation as well as for load sharing [1]. A microgrid that supplies to a rural area is widely spread and connected to many loads and distributed generators at different locations. In general, a DG may have local loads which are very close to it. There may be loads which are not near to any of the DGs and they must be shared by the DGs and the utility. These are termed as common load in this paper.

The most common method of local load sharing is the droop characteristics. Parallel converters have been controlled to deliver desired real and reactive power to the system. Local signals are used as feedback to control the converters, since in a real system, the distance between the converters may make an inter-communication impractical. The real and reactive power sharing can be achieved by controlling two independent quantities – the power angle, and the fundamental voltage magnitude [2-5]. The system stability during load sharing has been explored by many researchers [2, 4]. Transient stability of power system with high penetration level of power electronics interfaced (converter connected) distributed generation is explored in [3]. In [6], the operation of parallel-connected inverters with resistive output impedance of in an island microgrid is explored. The control loops are devised and analyzed, taking into account the special nature of a low-voltage microgrid. The feasibility of control strategies to be adopted for the operation of a microgrid when it becomes isolated is investigated in [7]. An evaluation of the need of storage devices and load shedding strategies is included in this paper.

The aim of this paper is to set up power electronics interfaced microgrid containing distributed generators. It is assumed that the common load is supplied solely by the utility in the grid connected mode. However, when an islanding occurs, this load will be shared by the DGs through traditional droop method. Furthermore, each DG will supply part of its local load in grid connected mode, while at the same time, compensating for their unbalance and nonlinearities. However in the islanded mode, each of the DGs supplies its local load and shares the common load through droop characteristics.

II. SYSTEM STRUCTURE

The basic power system model with two DGs is shown in Fig. 1 in which the real and reactive power drawn/supplied is denoted by P and Q respectively. The microgrid is connected to the utility grid at PCC. Both DG-1 and DG-2 are connected directly to the microgrid through circuit breaker CB-3 and CB-4 respectively. As mentioned in Section I, both the DGs have local loads which may be unbalanced and nonlinear. In addition, the microgrid may also have a common load, which is assumed to be balanced and linear and further away from any of the DGs. One of the functions of the DGs is to correct for the unbalance and nonlinearity of its local load. In the grid connected mode, the DGs share a percentage of its local load with the utility, while the common load is supplied entirely by the utility. During islanding, each DG supplies its local load and shares common load with the other DG. The complex powers drawn by the local loads are $P_{L1} + jQ_{L1}$ and $P_{L2} + jQ_{L2}$. The common load draws a current i_{LC} and a complex power of $P_{LC} + jQ_{LC}$. The local loads are connected to the DGs at PCC1 and PCC2 with voltages of v_{p1} and v_{p2} respectively. The real and reactive powers supplied by the DGs are denoted by P_1, Q_1 and P_2, Q_2. It is assumed that the microgrid is mostly resistive, being in the distribution level, with line impedances of R_{D1} and R_{D2}. The utility supply is denoted by v_s and the feeder resistance and inductance are denoted respectively by R_s and L_s. The utility supplies P_G and Q_G to the microgrid and the balance $P_s - P_G$ and $Q_s - Q_G$ are supplied to the utility load. The breakers CB-1 can isolate the microgrid from the utility supply.

The structure of the VSCs connecting DG-1 and DG-2 to the microgrid is shown in Fig. 2. Both the DGs are assumed to be ideal dc voltage sources V_{dc}. The compensator contains three H-bridge converters. The outputs of the H-bridges are connected to three single-phase transformers that are connected in wye for required isolation and voltage boosting [8]. The resistance R_f represents the switching and transformer losses, while the inductance L_f represents the leakage reactance of the transformers. The filter capacitor C_f is connected to the output of the transformers to bypass switching harmonics.

III. REFERENCE GENERATION AND COMPENSATOR CONTROL

In this section, the reference generation for the DG with compensator is presented. The control strategy for both the compensators is same. Here description is given only for DG-1 and its compensator.

A. Compensator Reference Generation in Grid Connected Mode

It is assumed, for the time being, that there is no common load and DG-2 (i.e., CB-2 and CB-4 are open), while DG-1 is supplying part of its local load only. The main aim of the compensator is to cancel the effects of unbalanced and harmonic components of the local load, while supplying pre-specified amount of real and reactive powers to the load. If it is successful in its aim, then current i_{g1} will be balanced and so will be the voltage v_{p1} provided that v_s is balanced. Let us denote the three phases by the subscripts a, b and c. Therefore since i_{g1} is balanced we have

$$i_{g1a} + i_{g1b} + i_{g1c} = 0 \tag{1}$$

From Fig. 1, the Kirchoff's current law (KCL) at v_{p1} gives

$$i_{1k} + i_{g1k} = i_{L1k}, \;\; k = a, b, c \tag{2}$$

Therefore combining (1) and (2) by adding the currents of the all the three phases together, we get

$$i_{1a} + i_{1b} + i_{1c} = i_{L1a} + i_{L1b} + i_{L1c} \tag{3}$$

Since i_{g1} is balanced due to the action of the compensator, the voltage v_{p1} will also become balanced. Hence the instantaneous real powers P_{G1} will be equal to its average component. Therefore we can write

$$v_{p1a} i_{g1a} + v_{p1b} i_{g1b} + v_{p1c} i_{g1c} = P_{G1} \tag{4}$$

From the KCL of (2), (4) can be written as

$$v_{p1a}\left(i_{L1a} - i_{1a}\right) + v_{p1b}\left(i_{L1b} - i_{1b}\right) + v_{p1c}\left(i_{L1c} - i_{1c}\right) = P_{G1} \tag{5}$$

Similarly the reactive powers Q_G will be equal to its instantaneous component, i.e.,

$$\left(v_{p1b}-v_{p1c}\right)i_{g1a}+\left(v_{p1c}-v_{p1a}\right)i_{g1b}+\left(v_{p1a}-v_{p1b}\right)i_{g1c}=\sqrt{3}\times Q_{G1} \tag{6}$$

Using the KCL of (2), (6) can be rewritten as

$$\left(v_{p1b}-v_{p1c}\right)\left(i_{L1a}-i_{1a}\right)+\left(v_{p1c}-v_{p1a}\right)\left(i_{L1b}-i_{1b}\right)+\left(v_{p1a}-v_{p1b}\right)\left(i_{L1c}-i_{1c}\right)=\sqrt{3}Q_{G1} \tag{7}$$

Equations (3), (5) and (7) form the basis of the algorithm. From these three, the following can be written

$$A\begin{bmatrix} i_{1a} \\ i_{1b} \\ i_{1c} \end{bmatrix}=A\begin{bmatrix} i_{L1a} \\ i_{L1b} \\ i_{L1c} \end{bmatrix}+\begin{bmatrix} 0 \\ -P_{G1} \\ -\sqrt{3}Q_{G1} \end{bmatrix} \tag{8}$$

where

$$A=\begin{bmatrix} 1 & 1 & 1 \\ v_{p1a} & v_{p1b} & v_{p1c} \\ v_{p1b}-v_{p1c} & v_{p1c}-v_{p1a} & v_{p1a}-v_{p1b} \end{bmatrix}$$

The determinant of the matrix A is given by

$$|A|=v_{p1a}\left(v_{p1c}+v_{p1b}-2v_{p1a}\right)+v_{p1b}\left(v_{p1a}+v_{p1c}-2v_{p1b}\right)+v_{p1c}\left(v_{p1b}+v_{p1a}-2v_{p1c}\right) \tag{9}$$

If v_{p1} is balanced, then the following is true

$$v_{p1a}+v_{p1b}+v_{p1c}=0 \tag{10}$$

Substituting (10) in (9), we get $|A| = -K$, where

$$K=3\left(v_{p1a}^2+v_{p1b}^2+v_{p1c}^2\right) \tag{11}$$

Then the solution of (8) is given as

$$\begin{bmatrix} i_{1a} \\ i_{1b} \\ i_{1c} \end{bmatrix}=\begin{bmatrix} i_{L1a} \\ i_{L1b} \\ i_{L1c} \end{bmatrix}-\frac{1}{K}\begin{bmatrix} 3P_{G1}v_{p1a}+\sqrt{3}Q_{G1}\left(v_{p1b}-v_{p1c}\right) \\ 3P_{G1}v_{p1b}+\sqrt{3}Q_{G1}\left(v_{p1c}-v_{p1a}\right) \\ 3P_{G1}v_{p1c}+\sqrt{3}Q_{G1}\left(v_{p1a}-v_{p1b}\right) \end{bmatrix} \tag{12}$$

As we have stipulated that DG-1 supplies a fraction of the average real and reactive power demanded by the local load, we can write

$$P_1 = \lambda_{1P} \times P_{L1av}$$
$$Q_1 = \lambda_{1Q} \times Q_{L1av} \tag{13}$$

where P_{L1av} and Q_{L1av} are respectively the average real and reactive power demanded by the local load and λ_{1P} and λ_{1Q} are respectively the real and reactive power fractions supplied by DG-1. It is to be noted that both the active and reactive powers will have double frequency and distorted components over the average components. DG-1 will supply the double frequency and distorted component to cancel out the unbalance and harmonics. Then, as a consequence, the active (P_{G1}) and reactive (Q_{G1}) power supplied by the grid will not contain any double frequency and distortion components. Additionally DG-1 will also supply a part of the average component.

Therefore the active and reactive power supplied by the grid is given by using the KCL of (2) as

$$P_{G1} = P_{L1av} - \lambda_{1P} \times P_{L1av} = P_{L1av}(1 - \lambda_{1P})$$
$$Q_{G1} = Q_{L1av} - \lambda_{1Q} \times Q_{L1av} = Q_{L1av}(1 - \lambda_{1Q}) \tag{14}$$

We can then modify (12) as to get the following reference currents for i_1

$$\begin{bmatrix} i_{1a} \\ i_{1b} \\ i_{1c} \end{bmatrix} = \begin{bmatrix} i_{L1a} \\ i_{L1b} \\ i_{L1c} \end{bmatrix} - \frac{1}{K} \begin{bmatrix} 3P_{L1av}(1-\lambda_{1P})v_{p1a} + \sqrt{3}Q_{L1av}(1-\lambda_{1Q})(v_{p1b} - v_{p1c}) \\ 3P_{L1av}(1-\lambda_{1P})v_{p1b} + \sqrt{3}Q_{L1av}(1-\lambda_{1Q})(v_{p1c} - v_{p1a}) \\ 3P_{L1av}(1-\lambda_{1P})v_{p1c} + \sqrt{3}Q_{L1av}(1-\lambda_{1Q})(v_{p1a} - v_{p1b}) \end{bmatrix} \tag{15}$$

In a similar way, the current references for DG-2 can be calculated and are given by

$$\begin{bmatrix} i_{2a} \\ i_{2b} \\ i_{2c} \end{bmatrix} = \begin{bmatrix} i_{L2a} \\ i_{L2b} \\ i_{L2c} \end{bmatrix} - \frac{1}{K} \begin{bmatrix} 3P_{L2av}(1-\lambda_{2P})v_{p2a} + \sqrt{3}Q_{L2av}(1-\lambda_{2Q})(v_{p2b} - v_{p2c}) \\ 3P_{L2av}(1-\lambda_{2P})v_{p2b} + \sqrt{3}Q_{L2av}(1-\lambda_{2Q})(v_{p2c} - v_{p2a}) \\ 3P_{L2av}(1-\lambda_{2P})v_{p2c} + \sqrt{3}Q_{L2av}(1-\lambda_{2Q})(v_{p2a} - v_{p2b}) \end{bmatrix} \tag{16}$$

Equations (15) and (16) will remain valid so long as DG-1 and DG-2 are supplying a part of their local loads and neither of the DGs is supplying the common load. When they will be required to supply the common load during islanding, (15) and (16) will be suitably modified to accommodate this. This will be discussed later in Section III.C.

B. Compensator Control

The equivalent circuit of one phase of the converter is shown in Fig. 3. In this, $u \cdot V_{dc1}$ represents the converter output voltage, where u is the switching function and is given by $u = \pm 1$. The main aim of the converter control is to generate u. From the circuit of Fig. 1, the following state vector is chosen

$$x^T = \begin{bmatrix} i_1 & i_{cf} & v_{p1} \end{bmatrix} \tag{17}$$

where the PCC voltage v_{p1} is the same as the voltage across the filter capacitor v_{cf}, i.e., $v_{cf} = v_{p1}$. Then the state space description of the system can be given as

$$\dot{x} = Ax + Bu_c \tag{18}$$

where u_c is the continuous time version of switching function u. The discrete-time equivalent of (18) is

$$x(k+1) = Fx(k) + Gu_c(k) \tag{19}$$

The control law is then given by

$$u_c(k) = -K\left[x(k) - x_{ref}(k)\right] \tag{20}$$

where K is a gain matrix and x_{ref} is the reference vector. The gain matrix, in this paper, is obtained through linear quadratic regulator (LQR) design. From $u_c(k)$, the switching function is generated as

$$\begin{aligned}&\text{If } u_c(k) > h \text{ then } u = +1\\&\text{elseif } u_c(k) < -h \text{ then } u = -1\end{aligned} \tag{21}$$

where h is a small number.

It is not required for the DG-1 and compensator to regulate the PCC1 voltage. However, this voltage is required as a reference in the state vector. Therefore the positive sequence of the fundamental of the PCC1 voltage is extracted as in [9] and it is used as the reference for v_{p1}. Also noting that the current i_{cf} is in quadrature with v_{p1}, its reference is computed by phase shifting the reference for v_{p1} by 90° and from the knowledge of the value of the filter capacitor C_f. The reference for the current i_1 can be obtained from (15). In exactly a similar fashion, DG-2 VSCs are controlled and its reference states are computed.

C. Compensator Reference Generation in Islanded Mode

In Section III.A, it has been assumed that the DGs are not required to supply the common load as it will be supplied by the utility. In case of an islanding, however, each of the DGs will have to supply its local load entirely. In addition, they must also share the real (P_{LC}) and reactive (Q_{LC}) power demand of the common load. Therefore in this mode, $\lambda_{1P} = \lambda_{1Q} = \lambda_{2P} = \lambda_{2Q} = 1$. Also P_{G1}, Q_{G1}, i_{g1}, P_{G2}, Q_{G2} and i_{g2} will be negative with respect to the directions shown in Fig. 1. If DG-1 supplies the local load P_{L1}, Q_{L1} and inject power $-P_{G1}$, $-Q_{G1}$ to the microgrid to share the common load then the total real and reactive power generated by the DG-1 are $P_1 = P_{L1} - P_{G1}$ and $Q_1 = Q_{L1} - Q_{G1}$.respectively. Similarly the total real and reactive power generated by the DG-2 are $P_2 = P_{L2} - P_{G2}$ and $Q_2 = Q_{L2} - Q_{G2}$.respectively.

Note from (15) and (16) that when $\lambda_{1P} = \lambda_{1Q} = \lambda_{2P} = \lambda_{2Q} = 1$, and the DGs also supply the grid currents, we have

$$\begin{bmatrix} i_{1a} \\ i_{1b} \\ i_{1c} \end{bmatrix} = \begin{bmatrix} i_{L1a} \\ i_{L1b} \\ i_{L1c} \end{bmatrix} + \begin{bmatrix} i_{g1a} \\ i_{g1b} \\ i_{g1c} \end{bmatrix} \text{ and } \begin{bmatrix} i_{2a} \\ i_{2b} \\ i_{2c} \end{bmatrix} = \begin{bmatrix} i_{L2a} \\ i_{L2b} \\ i_{L2c} \end{bmatrix} + \begin{bmatrix} i_{g2a} \\ i_{g2b} \\ i_{g2c} \end{bmatrix} \tag{22}$$

Following the derivations presented in (1) to (12) the injected currents are computed as

$$\begin{bmatrix} i_{g1a} \\ i_{g1b} \\ i_{g1c} \end{bmatrix} = -\frac{1}{K} \begin{bmatrix} 3P_{G1}v_{p1a} + \sqrt{3}Q_{G1}(v_{p1b} - v_{p1c}) \\ 3P_{G1}v_{p1b} + \sqrt{3}Q_{G1}(v_{p1c} - v_{p1a}) \\ 3P_{G1}v_{p1c} + \sqrt{3}Q_{G1}(v_{p1a} - v_{p1b}) \end{bmatrix} \text{and} \begin{bmatrix} i_{g2a} \\ i_{g2b} \\ i_{g2c} \end{bmatrix} = -\frac{1}{K} \begin{bmatrix} 3P_{G2}v_{p2a} + \sqrt{3}Q_{G2}(v_{p2b} - v_{p2c}) \\ 3P_{G2}v_{p2b} + \sqrt{3}Q_{G1}(v_{p2c} - v_{p2a}) \\ 3P_{G2}v_{p2c} + \sqrt{3}Q_{G1}(v_{p2a} - v_{p2b}) \end{bmatrix} \tag{23}$$

Therefore combining (22) and (23) we get the references for the islanded mode as

$$\begin{bmatrix} i_{1a} \\ i_{1b} \\ i_{1c} \end{bmatrix} = \begin{bmatrix} i_{L1a} \\ i_{L1b} \\ i_{L1c} \end{bmatrix} - \frac{1}{K} \begin{bmatrix} 3P_{G1}v_{p1a} + \sqrt{3}Q_{G1}(v_{p1b} - v_{p1c}) \\ 3P_{G1}v_{p1b} + \sqrt{3}Q_{G1}(v_{p1c} - v_{p1a}) \\ 3P_{G1}v_{p1c} + \sqrt{3}Q_{G1}(v_{p1a} - v_{p1b}) \end{bmatrix} \tag{24}$$

$$\begin{bmatrix} i_{2a} \\ i_{2b} \\ i_{2c} \end{bmatrix} = \begin{bmatrix} i_{L2a} \\ i_{L2b} \\ i_{L2c} \end{bmatrix} - \frac{1}{K} \begin{bmatrix} 3P_{G2}v_{p2a} + \sqrt{3}Q_{G2}(v_{p2b} - v_{p2c}) \\ 3P_{G2}v_{p2b} + \sqrt{3}Q_{G1}(v_{p2c} - v_{p2a}) \\ 3P_{G2}v_{p2c} + \sqrt{3}Q_{G1}(v_{p2a} - v_{p2b}) \end{bmatrix} \tag{25}$$

The generalized form for the reference currents of DG-1 can be given from (15) and (24) as

$$\begin{aligned} \begin{bmatrix} i_{1a} \\ i_{1b} \\ i_{1c} \end{bmatrix} = \begin{bmatrix} i_{L1a} \\ i_{L1b} \\ i_{L1c} \end{bmatrix} &- \frac{1}{K} \begin{bmatrix} 3P_{Lav1}(1-\lambda_{1P})v_{p1a} + \sqrt{3}Q_{Lav1}(1-\lambda_{1Q})(v_{p1b} - v_{p1c}) \\ 3P_{Lav1}(1-\lambda_{1P})v_{p1b} + \sqrt{3}Q_{Lav1}(1-\lambda_{1Q})(v_{p1c} - v_{p1a}) \\ 3P_{Lav1}(1-\lambda_{1P})v_{p1c} + \sqrt{3}Q_{Lav1}(1-\lambda_{1Q})(v_{p1a} - v_{p1b}) \end{bmatrix} \\ &- \frac{1}{K} \begin{bmatrix} 3P_{G1}(1-\lambda_{1PG})v_{p1a} + \sqrt{3}Q_{G1}(1-\lambda_{1QG})(v_{p1b} - v_{p1c}) \\ 3P_{G}(1-\lambda_{1PG})1v_{p1b} + \sqrt{3}Q_{G1}(1-\lambda_{1QG})(v_{p1c} - v_{p1a}) \\ 3P_{G1}(1-\lambda_{1PG})v_{p1c} + \sqrt{3}Q_{G1}(1-\lambda_{1QG})(v_{p1a} - v_{p1b}) \end{bmatrix} \end{aligned} \tag{26}$$

In the above equation, $\lambda_{1P} = \lambda_{1Q} = 1$ and $\lambda_{1PG} = \lambda_{1QG} = 0$ while sharing the common in the islanded mode, which will result in (24). However in the grid connected mode, when the local load is shared by the DG-1 and the grid, we have $0 < \lambda_{1P} \leq 1$ and $0 < \lambda_{1Q} \leq 1$ and $\lambda_{1PG} = \lambda_{1QG} = 1$. A similar expression as (26) can also be written for DG-2.

D. DG Coordination for Sharing the Common Load

From Fig. 1, it is clear that the total power demand from the common load P_{LC}, Q_{LC} is shared only by the DGs in the islanded mode. The KCL at PCC gives the following expression

$$i_{LC} = -i_{g1} - i_{g2} \tag{27}$$

Assuming that the microgrid is (almost) resistive, the active power balance equation at PCC is given from Fig. 1 by

$$P_{LC} = -P_{G1} - P_{G2} + \left|I_{g1}\right|^2 R_{D1} + \left|I_{g2}\right|^2 R_{D2} \tag{28}$$

where $|I_{g1}|$ and $|I_{g2}|$ are the rms values of i_{g1} and i_{g2} respectively. The reactive power balance equation at PCC is

$$Q_{LC} = -Q_{G1} - Q_{G2} \tag{29}$$

With respect to Fig. 1, let us define the rms voltage of the PCC as $|V_p|\angle\delta_p$ and that of the PCC1 as $|V_{p1}|\angle\delta_{p1}$. The real and reactive power flow from v_{p1} to v_p is then given as

$$-P_{G1} - jQ_{G1} = \left|V_p\right|\angle\delta_p \times \left[\frac{\left(\left|V_{p1}\right|\angle\delta_{p1} - \left|V_p\right|\angle\delta_p\right)}{R_{D1}}\right]^*$$

From the above equation, the real and reactive power is calculated as

$$\begin{aligned} -P_{G1} &= \frac{-\left|V_p\right|^2 + \left|V_{p1}\right|\left|V_p\right|\cos(\delta_p - \delta_{p1})}{R_{D1}} \\ -Q_{G1} &= \frac{\left|V_{p1}\right|\left|V_p\right|\sin(\delta_P - \delta_{P1})}{R_{D1}} \end{aligned} \tag{30}$$

When the angle difference $\delta_p - \delta_{p1}$ is small (30) can be rewritten as

$$\begin{aligned} -P_{G1} &= \frac{-\left|V_p\right|^2 + \left|V_{p1}\right|\left|V_p\right|}{R_{D1}} \Rightarrow -P_{G1} \propto \left(\left|V_p\right| - \left|V_{p1}\right|\right) \\ -Q_{G1} &= \frac{\left|V_{p1}\right|\left|V_p\right|(\delta_P - \delta_{P1})}{R_{D1}} \Rightarrow -Q_{G1} \propto \left(\delta_P - \delta_{P1}\right) \end{aligned} \tag{31}$$

Equation (31) gives us approximate relationships, which clearly indicate that the real and reactive power can be controlled by controlling the voltage magnitude ($|V_p| - |V_{p1}|$) and angle δ_{p1}. Therefore the real and reactive power output to the microgrid from the DG-1 can be controlled using their respective droop relations with the voltage magnitude and angle respectively. Since the voltage $|V_p|$ is not locally measurable, these are given by

$$\begin{aligned}\delta_{p1} &= \delta^*_{p1} - m_1 \times \left(Q_{G1} - Q^*_{G1}\right)\\ \left|V_{p1}\right| &= \left|V_{p1}\right|^* - n_1 \times \left(P_{G1} - P^*_{G1}\right)\end{aligned} \tag{32}$$

where $|V_{p1}|^*$, δ_{p1}^*, P_{G1}^* and Q_{G1}^* respectively are the rated values of the voltage magnitude, angle, real and reactive power. The coefficients m_1 and n_1 denote respectively the voltage magnitude and angle drop with real and reactive power output. These values are chosen to meet the voltage regulation requirement at point PCC1. In a similar way, the droop characteristics of DG-2 are given by

$$\begin{aligned}\delta_{p2} &= \delta^*_{p2} - m_2 \times \left(Q_{G2} - Q^*_{G2}\right)\\ \left|V_{p2}\right| &= \left|V_{p2}\right|^* - n_2 \times \left(P_{G2} - P^*_{G2}\right)\end{aligned} \tag{33}$$

In grid connected mode, discussed in Section III.B, the droop is inactive. Hence the reference voltage is set from the positive sequence fundamental component of the PCC1 (or PCC2) voltage. However, when the DGs are operating in the islanded mode, the magnitude and angle of the reference voltage are derived from the droop equations (32-33) given above. These are then used in the state feedback controller. Hence the positive sequence voltage extraction is unnecessary in this case and the nominal value before the islanding can be used in the droop equations. Once the voltage magnitude and angle from equations (32) and (33) are calculated, the current references are obtained from (24) and (25) respectively. Noting that each DG will have to supply its local load, the droop coefficients are chosen based on the ratings of the DGs. Neglecting the resistive drops across the microgrid, these are given by

$$\begin{aligned} n_1 \times \left(P_{1\_rated} - P_{L1\_\max}\right) &= n_2 \times \left(P_{2\_rated} - P_{L2\_\max}\right)\\ m_1 \times \left(Q_{1\_rated} - Q_{L1\_\max}\right) &= m_2 \times \left(Q_{2\_rated} - Q_{L2\_\max}\right)\end{aligned} \tag{34}$$

IV. SIMULATION STUDIES

Simulation studies are carried out in PSCAD/EMTDC (version 4.2) in which different configurations of load and its sharing are considered. The DGs are considered to be ideal dc sources. The system data are given in Table I. The numerical results of all the simulation studies are summarized and listed in Table II for better clarity.

A. Sharing the Local Load with Utility

In this section, the sharing of the local load by the DGs with utility is shown. In this case the current references of the DG compensators are calculated from (26) with $\lambda_{1PG} = \lambda_{1QG} = 1$ and $\lambda_{2PG} = \lambda_{2QG} = 1$ such that the DGs do not share the common load. It is desired that DG-1 shares 20% of both real and reactive power of its local load, while DG-2 shares 50% of the real power and 70% of the reactive power requirement of its own local load. So in this case $\lambda_{1P} = 0.2$, $\lambda_{1Q} = 0.2$ and $\lambda_{2P} = 0.5$, $\lambda_{2Q} = 0.7$. The common load is totally supplied by the utility. At 0.5 s, the common load impedance is made half of its initial value. Fig. 4 shows the power sharing of DG-1 and DG-2. The voltages of PCC1, PCC2 are shown in Fig. 5. The power sharing in same desired ratio and balanced voltages even after change in the common load indicate a stable operation.

To investigate the controller response in the islanded mode, with the same value of local and common loads, system is islanded at 0.4 s and, at the same time, the common load is also disconnected. As the island is detected, the each DG reference is changed to supply its total local load. A rapid island detecting scheme is introduced. The instantaneous power p_G injected by the grid is computed from the following relation

$$p_G = v_{pa} i_{ga} + v_{pb} i_{gb} + v_{pc} i_{gc} \tag{35}$$

Once this power falls below a threshold value, an islanding signal is generated. This instantaneous power p_G is used to detect the resynchronization when it rises above the threshold value. Fig. 6 (a) and (b) show the real and reactive power sharing of DG-1. Fig. 6 (c) and (d) show DG-1 current and voltages at PCC1. As soon as the islanding is detected at 0.4 s, the compensator current increases to deliver the total local load demand. A balanced voltage at PCC1 ensures proper functioning of the controller even after islanding. DG-2 also behaves in a similar fashion and its plots are not shown here.

B. Sharing the Common Load by the DGs

If the common load exists in the islanded mode, it is shared among the DGs proportional to their rating. It is desired to supply the real and reactive power from the DGs to their local load as before (as shown in Fig. 4). An islanding occurs at 0.3 s, where the common load remains connected. It is desired now that the local loads are totally supplied by the individual DGs and they share the common load as per (34). The droop coefficients of the DGs are taken such that they share the common load in 1:2 ratio in which DG-2 supplies 2/3rd of the load. Fig. 7 shows the real power sharing of DG-1 and DG-2. At the onset of the islanding, both PCC1 and PCC2 voltage drop, causing a slight drop in P_{L1} and P_{L2}. However both P_1 and P_2 increase to supply the common load, as indicated by negative power flow in P_{G1} and P_{G2}. At 1.0 s, the utility is reconnected and the power sharing goes back to the initial values.

C. Sharing a Common Induction Motor Load

An impedance load can absorb a sudden change in instantaneous real and reactive power like a infinite sink. However in case of a motor load, a sudden change in the terminal voltage gives large oscillation in real and reactive power level. To investigate the system response with the motor load, the common load shown in Fig. 1 is now replaced with an induction motor and the power sharing is observed by islanding and resynchronization the utility. Fig. 8 shows the results. The islanding and resynchronization occur at 0.2 s and 0.7 s respectively. During islanding it is desired that the motor load is shared between DGs in 1:2 ratio. The absolute value of common load supplied by the DGs along with the total motor load during islanded mode is indicated in Fig. 8. The system reaches steady state within 0.2 s after islanding and 0.3 s after resynchronization.

D. DG-1 Supplying the Entire Common Load during Islanding

Let us now assume that DG-2 is capable of supplying only its local load. Hence during an islanding, DG-1 must supply both its local load and the entire requirement of the common load. To investigate this operation an islanding is created at 0.25 s. Before islanding the following λ's are chosen:

$$\lambda_{1P} = 0.2,\ \lambda_{1Q} = 0.2 \text{ and } \lambda_{2P} = 1.0,\ \lambda_{2Q} = 1.0$$
$$\lambda_{1PG} = \lambda_{1QG} = \lambda_{2PG} = \lambda_{2QG} = 1.0$$

Once the islanding occurs, the following λ's are chosen:

$$\lambda_{1P} = 1.0,\ \lambda_{1Q} = 1.0,\ \lambda_{2P} = 1.0,\ \lambda_{2Q} = 1.0$$
$$\lambda_{1PG} = \lambda_{1QG} = 0 \text{ and } \lambda_{2PG} = \lambda_{2QG} = 1.0$$

The system response is shown in Fig. 9. Once the islanding occurs, there is a slight voltage drop in both PCC1 and PCC2, causing P_{L1} and P_{L2} to drop. DG-1 supplies its local and common load causing a rise in P_1 and negative P_{G1}. However DG-2 supplies only its local load, thereby maintaining P_{G2} to nearly zero.

V. DISCUSSIONS

In the studies presented in the paper, it has been assumed that only two DGs and a common load are connected to the microgrid. In general, however, there might be several DGs and loads connected to the microgrid as shown in Fig. 10. In this case a total number of *n* common loads and *m* DGs, with the compensators and local load are considered. The one way communication needed to broadcast the CB_grid status to the DG compensator is shown in Fig. 10. The total active and reactive powers consumed by the common loads are given by

$$\begin{aligned} P_{LC} &= P_{LC1} + P_{LC2} + \cdots + P_{LCn} \\ Q_{LC} &= Q_{LC1} + Q_{LC2} + \cdots + Q_{LCn} \end{aligned} \tag{36}$$

This total power will be supplied by the grid alone. However in islanded mode this power will be shared among the DGs. The power can be shared depending on the DG rating. Coefficient of the droop characteristics of the DGs should be chosen by

$$\begin{aligned} n_1 \times \left(P_{1\_rated} - P_{L1\_\max}\right) = n_2 \times \left(P_{2\_rated} - P_{L2\_\max}\right) = n_m \times \left(P_{m\_rated} - P_{Lm\_\max}\right) \\ m_1 \times \left(Q_{1\_rated} - Q_{L1\_\max}\right) = m_2 \times \left(Q_{2\_rated} - Q_{L2\_\max}\right) = m_m \times \left(Q_{m\_rated} - Q_{Lm\_\max}\right) \end{aligned} \tag{37}$$

However, similar to conventional droop method, the different line impedance between the load connection points throughout the microgrid will have impact on the load sharing. As the line impedances are not purely resistive or inductive, control of the active and reactive powers are not totally decoupled in nature. The detail impact of the line impedance on droop control is discussed in [10, 11].

VI. CONCLUSIONS

In this paper a local load sharing technique is proposed for a distributed microgrid. The controllers are capable of compensating the local unbalanced and non linear loads. The local loads can be shared with utility in any desired ratio. The common loads which are normally supplied by the utility in grid connected mode, shared among the DGs proportional to their rating in the islanded mode. A smooth transfer between the islanded and grid connected mode assures a stable operation of the system. The controller efficacy is checked both with impedance and motor loads. The application is mainly aimed at rural area where unbalanced load is common and wire less communication is always desirable due to the large network size. Similar to any droop control method, the distance among the load and DG determine the line impedance between them and that impedance has impact on the load sharing. However load sharing can be made more accurate by incorporating the line impedance values in the power reference calculation.

ACKNOWLEDGEMENT

The authors thank the Australian Research Council (ARC) for the financial support for this project through the ARC Discovery Grant DP 0774092.

REFERENCES

[1] Y. W. Li, D. M. Vilathgamuwa and P. C. Loh, “A grid-interfacing power quality compensator for three-phase three-wire microgrid applications,” IEEE Trans on Power Electronics, Vol. 21, Issue 4, pp. 1021-1031, July 2006.

[2] J. M. Guerrero, L. G. de Vicuna, J. Matas, M. Castilla, and J. Miret, "A wireless controller to enhance dynamic performance of parallel inverters in distributed generation systems," IEEE Trans on Power Electronics, Vol. 19, Issue 5, pp. 1205-1213, 2004.

[3] M. Reza, D. Sudarmadi, F. A. Viawan, W. L. Kling, and L. Van Der Sluis, "Dynamic Stability of Power Systems with Power Electronic Interfaced DG," in Power Systems Conference and Exposition, 2006. PSCE '06. 2006 IEEE PES, 2006, pp. 1423-1428.

[4] M. C. Chandorkar, D. M. Divan and R. Adapa, “Control of parallel connected inverters in standalone ac supply systems,” IEEE Trans. on Industry Applications, Vol. 29, No. 1, pp. 136-143, 1993.

[5] F. Katiraei and M. R. Iravani, "Power Management Strategies for a Microgrid with Multiple Distributed Generation Units," IEEE Trans on Power Systems, Vol. 21, Issue 4, pp. 1821-1831, 2006.

[6] J. M. Guerrero, J. Matas, L. G. de Vicuna, M. Castilla, and J. Miret, “Decentralized control for parallel operation of distributed generation inverters using resistive output impedance,” IEEE Trans. on Industrial Electronics, Vol. 54, Issue 2, pp.994-1004, April 2007.

[7] J.A.P. Lopes, C.L. Moreira, A.G. Madureira, “Defining control strategies for MicroGrids islanded operation” IEEE Trans on Power System, Vol. 21, Issue 2, May 2006 pp.916-924.

[8] A. Ghosh and A. Joshi, “A new approach to load balancing and power factor correction in power distribution system,” IEEE Trans. on Power Delivery, Vol. 15, Issue 1, pp. 417-422, 2000**.**

[9] A. Ghosh and G. Ledwich, “Load compensating DSTATCOM in weak ac systems,” IEEE Trans. Power Delivery, Vol. 18, Issue 4, pp. 1302-1309, 2003.

[10] A. Tuladhar, H. Jin, T. Unger, and K. Mauch, “Parallel operation of single phase inverters with no control interconnections,” Proc. IEEE APEC’97, Vol. 1, pp. 94-100, 1997.
[11] A. Tuladhar, H. Jin, T. Unger, and K. Mauch, “Control of Parallel Inverters in Distributed AC Power Systems with Consideration of Line Impedance Effect,” IEEE Trans. on Industry Applications, Vol. 36, Issue 1, pp. 131-138, 2000.

Table-I: System Parameters

System Quantities	**Values**
Systems frequency	50 Hz
Source voltage (V_s)	11 kV rms (L-L)
Feeder impedance	R_s = 1.025 Ω, L_s = 57.75 mH
DG-1 Local Unbalanced load	R_{La} = 48.4 Ω, L_{La} = 192.6 mH R_{Lb} = 24.4 Ω, L_{Lb} = 100.0 mH R_{Lc} = 96.4 Ω, L_{Lc} = 300.0 mH
DG-1 Local Nonlinear load	A three-phase rectifier supplying an RL load with R = 200 Ω, L = 100 mH
DG-2 Local Unbalanced load	R_{La} = 48.4 Ω, L_{La} = 192.6 mH R_{Lb} = 24.4 Ω, L_{Lb} = 100.0 mH R_{Lc} = 96.4 Ω, L_{Lc} = 300.0 mH
DG-2 Local Nonlinear load	A three-phase rectifier supplying an RL load with R = 200 Ω, L = 100 mH
Common Impedance Load	R_{La} = 24.4 Ω, L_{La} = 100.0 mH R_{Lb} = 24.4 Ω, L_{Lb} = 100.0 mH R_{Lc} = 24.4 Ω, L_{Lc} = 100.0 mH
Common Motor Load (M)	Induction motor rated 40 hp, 11 kV rms (L-L).
Microgrid Line Impedance	R_{D1}=R_{D2}=0.2 Ω
DGs and Compensators DC voltage (V_{dc1}) Transformer rating VSC losses Filter Capacitance (C_f)	 3.5 kV 3 kV/11 kV, 0.5 MVA, 2.5% reactance (L_f) 1.5 Ω 50 μF
Droop Coefficients m_1 m_2 n_1 n_2	 - 0.1 rad/MVAr - 0.05 rad/MVAr 0.12 kV/MW 0.06 kV/MW

Table-II: Numerical Results

		Active Power	Initial value (MW)	Final value (MW)	Reactive Power	Initial value (MVAr)	Final value (MVAr)
Section IV.A: Sharing the Local Load with Utility	Fig.4	P_1	0.275	0.274	Q_1	0.28	0.28
		P_{G1}	1.125	1.125	Q_{G1}	1.12	1.12
		P_{L1}	1.4	1.39	Q_{L1}	1.4	1.4
		P_2	0.71	0.69	Q_2	0.42	0.41
		P_{G2}	0.69	0.69	Q_{G2}	0.18	0.17
		P_{L2}	1.4	1.38	Q_{L2}	0.6	0.58

		Voltage drop at PCC1 (%)	Voltage drop at PCC2 (%)
Section IV.A	Fig.5	3.15%	3.38%

		Active Power	Initial value (MW)	Final value (MW)	Reactive Power	Initial value (MVAr)	Final value (MVAr)
Section IV.A	Fig.6	P_1	0.142	0.71	Q_1	0.09	0.43
		P_{G1}	0.568	0.0	Q_{G1}	0.36	0.0
		P_{L1}	0.71	0.69	Q_{L1}	0.45	0.43

		Active Power	Initial value (MW)	Intermediate value (In Islanded Mode) (MW)	Final value (After resynchronization) (MW)
Section IV.B: Sharing the Common Load by the DGs	Fig.7	P_1	0.142	0.78	0.142
		P_{G1}	0.568	-0.13	0.568
		P_{L1}	0.71	0.65	0.71
		P_2	0.35	0.91	0.35
		P_{G2}	0.35	-0.31	0.35
		P_{L2}	0.70	0.60	0.70

		Active And Reactive Power	Initial value (Active power in MW and reactive power in MVAr)	Intermediate value (In Islanded Mode) (Active power in MW and reactive power in MVAr)	Final value (After resynchronization) (Active power in MW and reactive power in MVAr)
Section IV.C: Sharing a Common Induction Motor Load	Fig.8	P_{G1}	0.95	-.081	0.95
		P_{G2}	0.60	-0.157	0.60
		P_{LC}	0.238	0.238	0.238
		Q_{G1}	0.59	-0.039	0.59
		Q_{G2}	0.21	-0.076	0.21
		Q_{LC}	0.115	0.115	0.115

		Active Power	Initial value (MW)	Final value (In Islanded Mode) (MW)
Section IV.D: DG-1 Supplying the Entire Common Load During Islanding	Fig.9	P_1	0.34	1.86
		P_{G1}	1.50	-0.28
		P_{L1}	1.83	1.58
		P_2	1.825	1.625
		P_{G2}	0.01	-0.025
		P_{L2}	1.835	1.6

		Voltage Drop at PCC1 (%)	Voltage Drop at PCC2 (%)
Section IV.D	Fig.9	4.3%	5.8%

Figure Captions

Fig. 1. The microgrid and utility system under consideration.

Fig. 2. DG connection to the microgrid through three single-phase VSCs.

Fig. 3. Equivalent circuit of one phase of the converter.

Fig. 4. Real and reactive power sharing in DG-1and DG-2.

Fig. 5. Voltages at the PCC1 and PCC2.

Fig. 6. Power sharing and DG-1current and PCC1 voltages.

Fig. 7. Real power sharing by DG-1 and DG-2.

Fig. 8. Common load sharing between DG-1 and DG-2.

Fig. 9. Real power sharing of the DGs and voltages at PCC1 and PCC2.

Fig. 10. Microgrid structure with large number of DGs and loads.

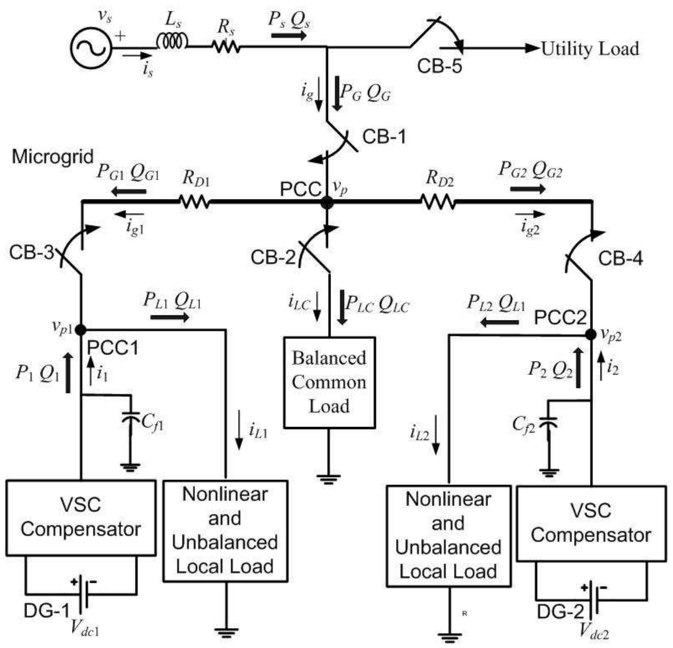

Fig.1. The microgrid and utility system under consideration.

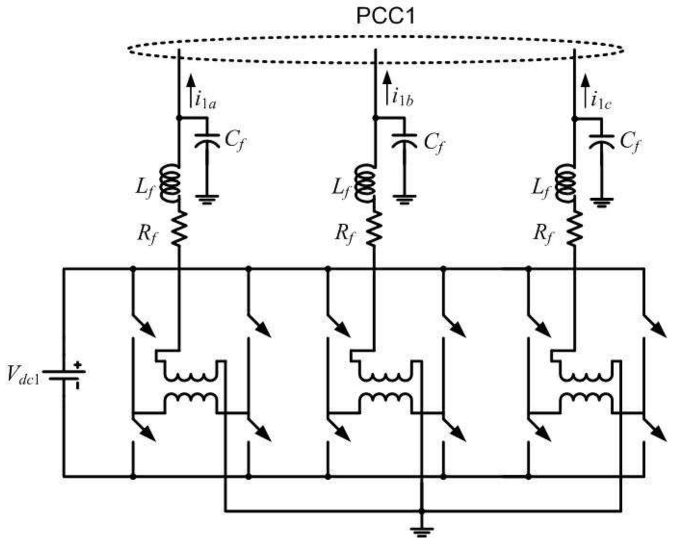

Fig.2. DG connection to the microgrid through three single-phase VSCs.

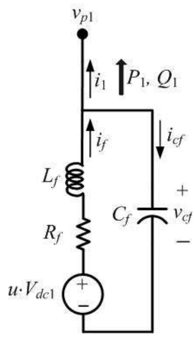

Fig. 3. Equivalent circuit of one phase of the converter.

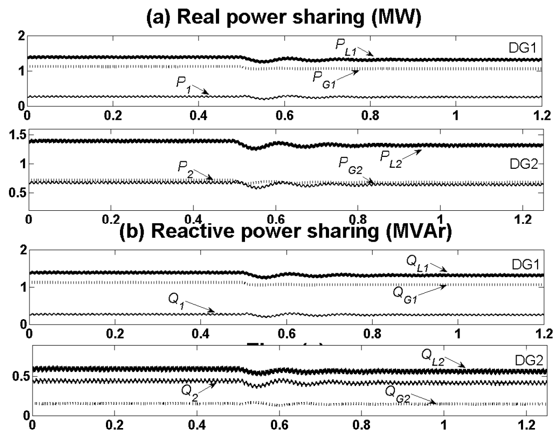

Fig.4. Real and reactive power sharing in DG-1and DG-2

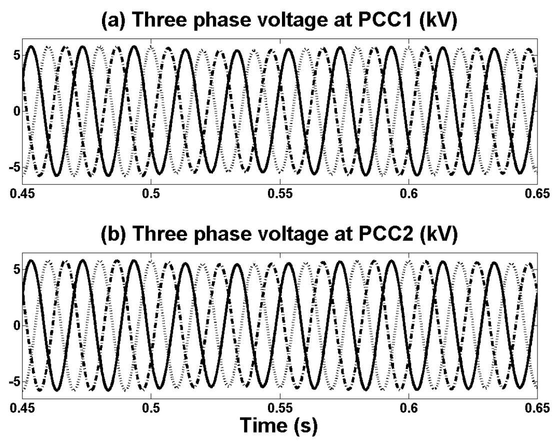

Fig.5. Voltages at the PCC1 and PCC2

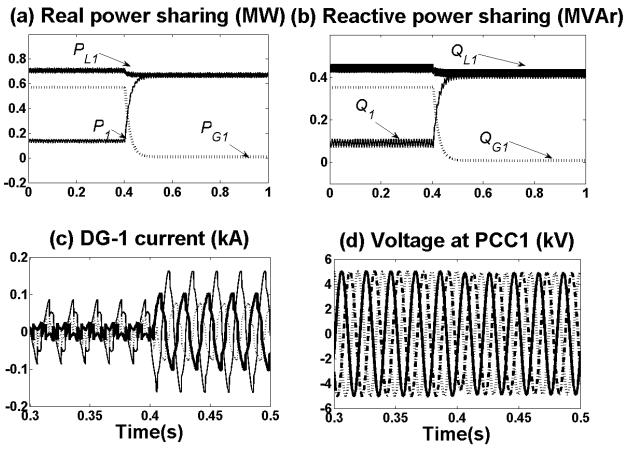

Fig.6. Power sharing and DG-1current and PCC1 voltages

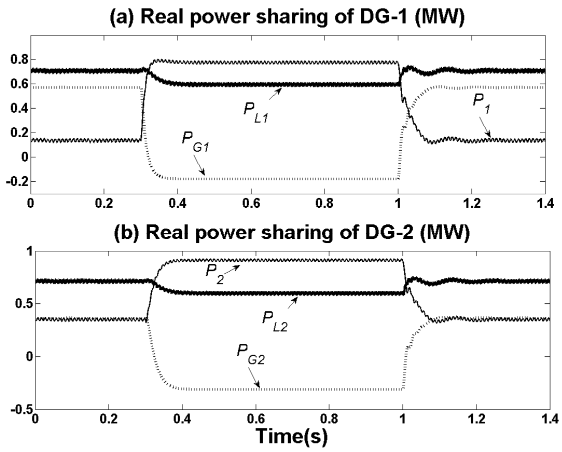

Fig.7. Real power sharing by DG-1 and DG-2.

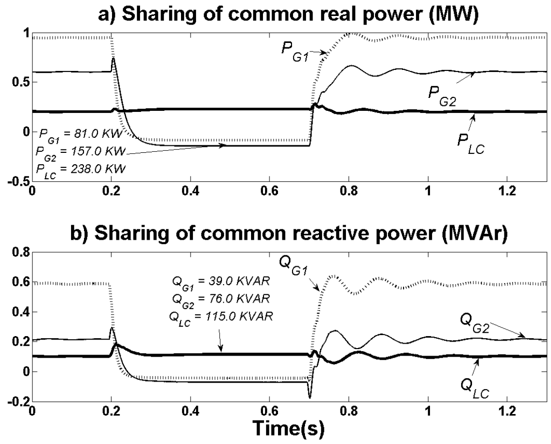

Fig. 8. Common load sharing between DG-1 and DG-2

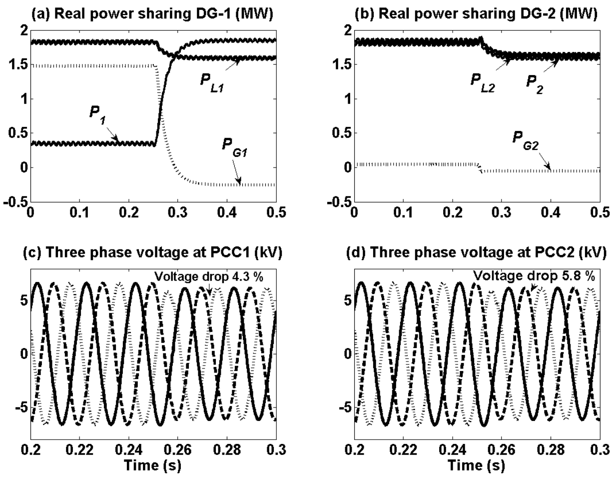

Fig.9. Real power sharing of the DGs and voltages at PCC1 and PCC2

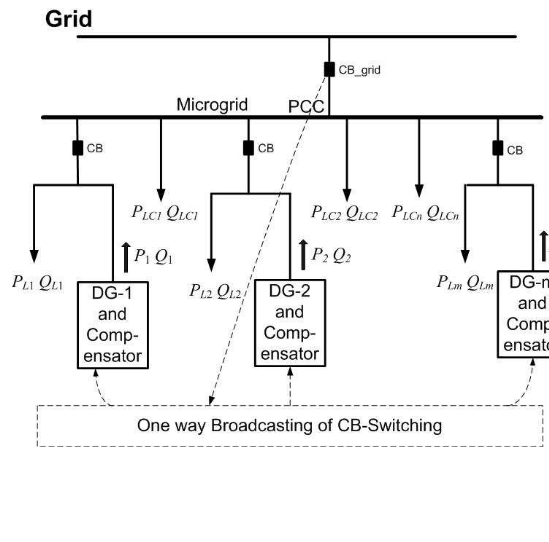

Fig.10. Microgrid structure with large number of DGs and loads.